

Efficient removal of insecticide “imidacloprid” from water by electrochemical advanced oxidation processes

Meral Turabik · Nihal Oturan · Belgin Gözmen · Mehmet A. Oturan

Received: 19 February 2014 / Accepted: 10 March 2014 / Published online: 27 March 2014
© Springer-Verlag Berlin Heidelberg 2014

Abstract The oxidative degradation of imidacloprid (ICP) has been carried out by electrochemical advanced oxidation processes (EAOPs), anodic oxidation, and electro-Fenton, in which hydroxyl radicals are generated electrocatalytically. Carbon-felt cathode and platinum or boron-doped diamond (BDD) anodes were used in electrolysis cell. To determine optimum operating conditions, the effects of applied current and catalyst concentration were investigated. The decay of ICP during the oxidative degradation was well fitted to pseudo-first-order reaction kinetics and absolute rate constant of the oxidation of ICP by hydroxyl radicals was found to be $k_{abs(ICP)} = 1.23 \times 10^9 \text{ L mol}^{-1} \text{ s}^{-1}$. The results showed that both anodic oxidation and electro-Fenton process with BDD anode exhibited high mineralization efficiency reaching 91 and 94 % total organic carbon (TOC) removal at 2 h, respectively. For Pt-EF process, mineralization efficiency was also obtained as 71 %. The degradation products of ICP were identified and a plausible general oxidation mechanism was proposed. Some of the main reaction intermediates such as 6-chloronicotinic acid, 6-chloronicotinaldehyde, and 6-hydroxynicotinic acid were determined by GC-MS analysis. Before complete mineralization, formic, acetic, oxalic, and glyoxylic acids were identified as end-products. The initial chlorine and organic

nitrogen present in ICP were found to be converted to inorganic anions Cl^- , NO_3^- , and NH_4^+ .

Keywords Anodic oxidation · Electro-Fenton · Imidacloprid · Reaction intermediates · Hydroxyl radicals · Water treatment

Abbreviations

ICP	Imidacloprid
EF-Pt	Pt anode/carbon felt cathode cell
BDD	Boron-doped diamond
EF-BDD	BDD anode/carbon felt cathode cell
AO-BDD	Anodic oxidation with BDD anode/carbon felt cathode with H_2O_2 production
TOC	Total organic carbon

Introduction

The continued exponential growth in human population gave out a corresponding increase to demands for agricultural products and freshwater. Therefore, in order to supply this huge need, a wide variety and quantity of pesticides have been used in the last century. The United Nations estimate that of all pesticides used in agriculture, less than 1 % actually reaches the crops (Kopling et al. 1996). The remaining percentage contaminates the land, air, and especially, water that can directly threaten the health of aquatic organisms and humans (Kopling et al. 1996; Meyer and Thurman 1996; Banks et al. 2005). Pesticides are known, in a large part, to be toxic, chemically stable, and recalcitrant to biological treatment. They are considered to be persistent organic pollutants and accumulate in water, air, and soil that cause risks of long-term toxicity (Zapata et al. 2010; Rouvalis et al. 2009). Because of these health and environmental risks, pesticides have been appointed as priority

Responsible editor: Philippe Garrigues

M. Turabik · N. Oturan · M. A. Oturan
Laboratoire Géomatériaux et Environnement (LGE), Université Paris-Est, EA 4508, UPEMLV, 77454 Marne-la-Vallée, France

M. Turabik (✉)
Technical Science Vocational School, Chemical Program, Mersin University, 33343 Mersin, Turkey
e-mail: turabikm@hotmail.com

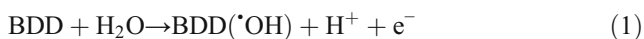
B. Gözmen
Department of Chemistry, Arts and Sciences Faculty, Mersin University, 33343 Mersin, Turkey

substances in EU legislation (EU Directive 2000). Therefore, in order to reduce/eliminate the harmful effects of pesticides on the non-target organisms, there is a need to develop efficient, feasible, and cost-effective water treatment techniques that promote the removal of these pollutants from water.

In recent years, the advanced oxidation processes (AOPs) have been attracting amazing attention for the treatment of organic pollutants in aqueous solution up to the mineralization stage (Ozcan et al. 2009; Brillas et al. 2009). These processes, based on the chemistry of hydroxyl radicals ($\cdot\text{OH}$), are currently used for the destruction of toxic and/or persistent organic pollutants. Hydroxyl radical is a powerful oxidizing agent ($E^\circ=2.80$ V/NHE) and react in a non-selective way on organic compounds leading finally to the mineralization end-products. AOPs, such as Fenton ($\text{Fe(II)/H}_2\text{O}_2$), photo-Fenton ($\text{Fe(II)/H}_2\text{O}_2/\text{UV}$), and heterogeneous photocatalysis (UV/TiO_2) have already been identified as a potential option to remove pesticides from contaminated water (Benitez et al. 2007; Martins et al. 2007). Hydroxyl radicals allow the oxidative degradation of organic pollutants until their mineralization into CO_2 and H_2O . Since $\cdot\text{OH}$ production does not involve the use of harmful chemicals which can be hazardous for the environment, this process is considered environmentally friendly for wastewater treatment and seems to be promising for the treatment of water contaminated by persistent and/or toxic organic pollutants (Diagne et al. 2007; Ozcan et al. 2008; Flox et al. 2006).

Recently, new electrochemical advanced oxidation processes (EAOPs) were proposed as alternative processes according to their environmental suitability, high effectiveness, fast treatment rate, and safety which related to moderately working conditions (Brillas et al. 2009; Nidheesh and Gandhimathi 2012). They are based on direct or indirect electrochemical generation of $\cdot\text{OH}$ (Brillas et al. 2009; Oturan 2000).

In the present work, the oxidative degradation/mineralization of a systemic insecticide imidacloprid (ICP) has been carried out by EAOPs; anodic oxidation and electro-Fenton using both Pt and boron-doped diamond (BDD) anodes. In the anodic oxidation (AO) process, oxidation of organic pollutants takes place in two ways: direct electron transfer to the anode (M) and/or chemical oxidation with $\text{M}(\cdot\text{OH})$ formed by oxidation of water on a high-overvoltage anode like BDD (Martínez-Huitle and Ferro 2006; Panizza and Cerisola 2009; Marselli et al. 2003; Michaud et al. 2003). BDD anode is able to produce high amounts of weakly adsorbed and highly reactive hydroxyl radicals ($\text{BDD}(\cdot\text{OH})$) from reaction (1):

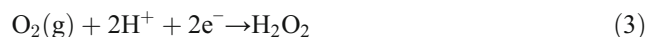


Although in the case of the electro-Fenton (EF) process, $\cdot\text{OH}$ is produced indirectly in the homogeneous

medium from electrocatalytically in situ generated Fenton's reagents (reaction (2)):



H_2O_2 is continuously generated in a contaminated acidic solution from the two-electron reduction of O_2 at a carbonaceous cathode. The carbon felt cathode constitutes one of the most used due to its large active surface area, simplicity, low cost, and outstanding performance, which is mainly due to the ability to produce H_2O_2 and efficient cathodic regeneration of the Fe^{2+} catalyst following reactions (3) and (4), respectively (Oturan et al. 2008; Sirés et al. 2008).



When BDD is used as anode in EF, degradation of organic pollutants is performed both at the anode surface by heterogeneous $\text{BDD}(\cdot\text{OH})$ formed from reaction (1) in the bulk solution by homogeneous $\cdot\text{OH}$ generated from reaction (2).

In this study, we chose the insecticide ICP as a model pollutant to be removed from water. ICP is a systemic insecticide belonging to chemical family "neonicotinoids" that act on the central neuron system of insects. ICP is commercially developed and marketed in the early to mid-1990s. It is a general-use pesticide utilized worldwide for crop, fruit, and vegetable pest control and termite and flea control in dogs and cats (Ishii et al. 1994; Cox 2001). The extensive use of ICP results in the increase of the environmental threats due to its relatively high solubility (0.58 g L^{-1}), stability in water and low degradation by photolysis (Cox 2001; Moza et al. 1998; Wamhoff and Schneider 1999). ICP is reported as an unlikely carcinogen and toxic to animals and aquatic fauna and flora (Suchail et al. 2011; Endocrine disruptor Screening Program: Tier 1 Screening Order Issuing Announcement. Federal Register Notice, Oct 21 2009). It is one of the most toxic insecticides to bees with acute toxicity ranging between 0.0005 to 0.007 μg acute inhalation (a.i.) per bee. The acute toxicity (C_{L50}) for alga and fishes is about 9 and 82 mg L^{-1} . Because of all these risks and side effects, it is important to develop efficient technologies to remove ICP from water. Recently, some methods have been applied for its removal from aqueous solutions such as biotransformation (Pandey et al. 2009), biodegradation (Anhalt et al. 2007), adsorption (Zahoor and Mahramanlioglu 2011; Daneshvar et al. 2007), photolysis (Moza et al. 1998; Dell'Arciprete et al. 2009; Scippers and Schwack 2008; Malato and Caceres 2001), and rather advanced oxidation processes: photocatalytic degradation (Malato and Caceres 2001; Cernigoi et al. 2007; Mahmoodi et al. 2007; Guan et al. 2008; Kitsiou et al. 2009), photo-electrocatalytic degradation (Philippidis et al.

2009), ozonation (Bourgin et al. 2011), photo-Fenton (Malato and Caceres 2001; Segura et al. 2008), solar photo-Fenton (Zapata et al. 2009). Although several methods had been applied to degradation of ICP and some of intermediates were determined during its degradation no work has been done by using EAOPs.

The degradation of ICP was carried out by using different configuration of EF process: Pt anode/carbon felt cathode (EF-Pt), BDD anode/carbon felt cathode (EF-BDD) and anodic oxidation with BDD anode/carbon felt cathode (AO-BDD) with H₂O₂ generation. The effects of some important reaction parameters such as electrical current, catalyst concentration, and anode material were evaluated. The kinetics of oxidation reactions and mineralization efficiencies of EAOPs were investigated. The aromatic and aliphatic intermediates as well as inorganic ions released during the treatments were identified. Using all these data and TOC removal results, a plausible mineralization pathway of ICP by [•]OH was proposed.

Experimental

Chemicals

The ICP, 1-(6-chloro-3-pyridylmethyl)-N-nitroimidazolidin-2-ylideneamine (C₉H₁₀ClN₅O₂) was obtained from Sigma-Aldrich (99.9 % purity). Its chemical structure and physico-chemical properties were given in Table 1. The catalyst source chemical, FeSO₄·7H₂O and supporting electrolyte chemical Na₂SO₄ were obtained from Acros with 99.9 % purity. H₃PO₄ and CH₃OH, used for preparation of mobile phase in HPLC, were obtained from Sigma-Aldrich. The 4-hydroxybenzoic acid (4-HBA), which was used as a standard competitor in rate constant determination, was obtained from Acros Organics. Formic, oxalic, glyoxylic, and acetic acids were purchased from Sigma-Aldrich and Fluka. H₂SO₄, NaHCO₃,

Na₂CO₃, NaNO₃, NaCl, and (NH₄)₂C₂O₄ employed in ion chromatography were analytical grade and obtained from Fluka and Acros Organics.

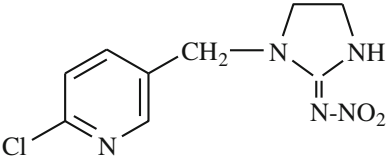
The water used in the preparation of the solutions and eluents in HPLC and liquid chromatography-electrospray ionization-tandem mass spectrometry (LC/ESI-MS/MS) analyses was obtained from a Millipore Milli-Q (simplicity 185) system with resistivity of >18 MΩ cm.

Electrochemical cell and apparatus

A one-compartment electrochemical cell with a stabilized power supply was used for the oxidative degradation experiments. Carbon felt electrode that has a 3D shape and 60-cm² physical surface area was used as a cathode (Carbone Lorraine, France). The anodes were Pt and BDD. The Pt anode was a cylindrical grid of 4.5 cm of height and 3 cm of internal diameter. The BDD anode was a 24-cm² thin film deposited on a niobium substrate (CONDIAS, Germany). In all cases, the anode was set up in the center of the electrochemical cell and the carbon felt cathode was established in the inner wall of the cell.

The concentration decay of ICP during the oxidative degradation, was followed by HPLC analysis at λ=269 nm using a Merck LaChrom chromatograph equipped with a diode array detector (model DAD L-7455). The reversed-phase column (Purospher RP-18, 5 μm, 4.6×250 mm, Merck) at 35 °C was used in analysis. In all cases, 20 μL of sample volume was injected into the HPLC. The 0.1 % phosphoric acid–methanol (70:30 v/v) mixture was used as mobile phase at a flow rate of 0.8 mL min⁻¹. ICP displays a well-defined peak at the retention time of 11.6 min under above mentioned conditions. The identification of carboxylic acids formed during the degradation of ICP was carried out by the same HPLC chromatograph at 210 nm using a 300-mm SUPELCOGEL H column (ϕ=7.8) with a mobile phase of 4-mM H₂SO₄.

Table 1 Chemical structure and physicochemical properties of ICP

Chemical structure	Chemical formula	Molecular weight (g mol ⁻¹)	Water solubility (mg L ⁻¹ , 20 °C, pH 7)	Soil adsorption coefficient
	C ₉ H ₁₀ ClN ₅ O ₂	255.7	514	K _d : 0.956-4.18 K _{oc} : 132-310

Oxidation reaction intermediates were analyzed by HPLC, GC/MS, and LC/ESI-MS/MS techniques. Agilent LC/ESI-MS/MS system consist of a binary LC pump, an autosampler, and a temperature-controlled column oven of Agilent series 1200 and an Agilent 6460 triple quadrupole mass spectrometer equipped with an electrospray ionization + jet stream performance interface. Experimental conditions were as follows: drying gas (N_2 , 20 psig) flow of 10 L min^{-1} , nebulizer pressure of 45 psig, drying gas temperature of $300\text{ }^\circ\text{C}$, and capillary voltage of 2,000 V. The analytical separation was performed on an Agilent XDB-C18 column ($4.6\times 50\text{ mm}$, $1.8\text{ }\mu\text{m}$) using isocratic elution of 70 % H_2O containing 2-mM NH_4CH_3COO and 30 % MeOH at a flow rate of 0.5 mL min^{-1} at $25\text{ }^\circ\text{C}$. The MS detector was operated in the positive mode with mass detection in the range from 50 to 800 amu.

The GC-MS analysis was performed using a 5890A Agilent model gas chromatograph with an auto-injector and interfaced with ECD, NPD, and 5975C mass selective detector. The aqueous solutions were extracted three times with 50 mL of ethyl acetate. The $3\text{ }\mu\text{L}$ of sample was analyzed in GC-MS. An HP5-MS capillary column ($30\text{ m}\times 0.25\text{ mm}\times 0.25\text{ }\mu\text{m}$) was used as analytical column. Helium was used as the carrier gas with a flow rate of 2 mL min^{-1} . The GC injection port temperature was set at $280\text{ }^\circ\text{C}$ (split mode=1/40), and the column temperature was fixed at $50\text{ }^\circ\text{C}$ for 2 min. Subsequently, the column was sequentially heated at a rate of $5\text{ }^\circ\text{C/min}$ to $300\text{ }^\circ\text{C}$ and held for 10 min at this temperature. The MS detector was operated in the EI mode (70 eV).

The mineralization efficiency of the ICP solutions was determined with total organic carbon (TOC) analysis using a Shimadzu TOC-VSCH analyzer. The oxygen was used as carrying gas with a flow rate of 150 mL min^{-1} . Pt was used as a catalyst in order to enhance the combustion reaction. The injection volumes were $50\text{ }\mu\text{L}$ and oven temperature was $680\text{ }^\circ\text{C}$.

Dionex ICS-1000 Basic Ion Chromatography System, controlled by Chromeleon SE software was used for analysis of released inorganic ions (Cl^- , NO_3^- , and NH_4^+) during the treatment. For anions analysis, anion-exchange column (IonPac AS4ASC, $25\text{ cm}\times 4\text{ mm}$) was linked to an IonPac AG4A-SC, $5\text{ cm}\times 4\text{ mm}$ column guard. For cations analysis, cation-exchange column (IonPac CS12A, $25\text{ cm}\times 4\text{ mm}$) was linked to an IonPac CG12A, $5\text{ cm}\times 4\text{ mm}$ column guard. The system was equipped with a DS6 conductivity detector containing a cell heated at $35\text{ }^\circ\text{C}$. An ASRS-ULTRA II (for anions) or CSRS-ULTRA II (for cations) self-regenerating suppressor was used to improve the sensitivity of the detector. A solution of 1.8-mM Na_2CO_3 and 1.7-mM $NaHCO_3$ at 2.0 mL min^{-1} , and a 9.0-mM H_2SO_4 solution at 1.0 mL min^{-1} were used as mobile phases for anion and cation analysis, respectively.

Experimental procedure

The oxidative degradation of 200-mL volumes of 0.1-mM ICP aqueous solutions was performed by the electro-Fenton (EF) process using the following configurations: Pt anode/carbon felt cathode (EF-Pt), BDD anode/carbon felt cathode (EF-BDD) and by the anodic oxidation with BDD anode/carbon felt cathode (AO-BDD). In EF experiments, 0.2-mM Fe^{2+} (from $FeSO_4\cdot 7H_2O$) was used as catalyst in a 50-mM Na_2SO_4 aqueous solution. The value of pH constitutes one of the important operating parameters in EF process. It is signed out in the literature that the pH 3.0 is the optimum value to carry out the Fenton's reaction and related processes like EF (Brillas et al. 2009; Diagne et al. 2007; Sirés et al. 2006; Daneshvar et al. 2008). At this pH, the predominant iron species is present in $Fe(OH)^{2+}$ form (Boye et al. 2002). Thus, the initial pH of the ICP aqueous solutions was adjusted to pH 3.0 in EF-Pt and EF-BDD systems. AO-BDD experiments were carried out at the natural pH (about 5.6) of the ICP solution. Na_2SO_4 aqueous solution (50 mM) was used as supporting electrolyte. But, ferrous ion was not added in the solution. Before starting the processes, ICP solutions were saturated with O_2 gas by bubbling compressed air having passed through a frit with a flow rate of 1 L min^{-1} for 10 min. Two milliliters of ICP samples were taken before all electrolysis. Samples were taken at pre-determined time intervals (2, 5, 7, 10, 15, 20, 30, 40, 50, 60, 90, 120, 240, 360, 480 min) for analyses.

Results and discussion

Degradation kinetics of ICP

To determine optimum catalyst dose and applied current value, experiments at various initial Fe^{2+} concentrations (0.05, 0.1, 0.2, 0.5, and 1.0 mM) were conducted in EF-Pt cell. Then, the effect of current intensity was investigated at various constant current values ($I=50, 100, 200, 300, 400, 500$, and 1.000 mA) for EF-Pt, EF-BDD, and AO-BDD cells.

Effect of applied current on ICP decay

The value of the applied current is an important parameter in the EF process, since it determines the formation rate of H_2O_2 (reaction (3)) and regeneration rate of Fe^{2+} from Fe^{3+} ions (reaction (4)), and consequently, the formation rate of $\cdot OH$ following the Fenton reaction (2). Therefore, the effect of the applied current on the oxidative degradation rate of ICP was examined by using various applied current values (50, 100, 200, 300, 400, 500, and 1,000 mA) in EF-Pt, EF-BDD, and AO-BDD cells. The concentration decay results of ICP in EF-Pt, EF-BDD, and AO-BDD were given in Fig. 1. In case of

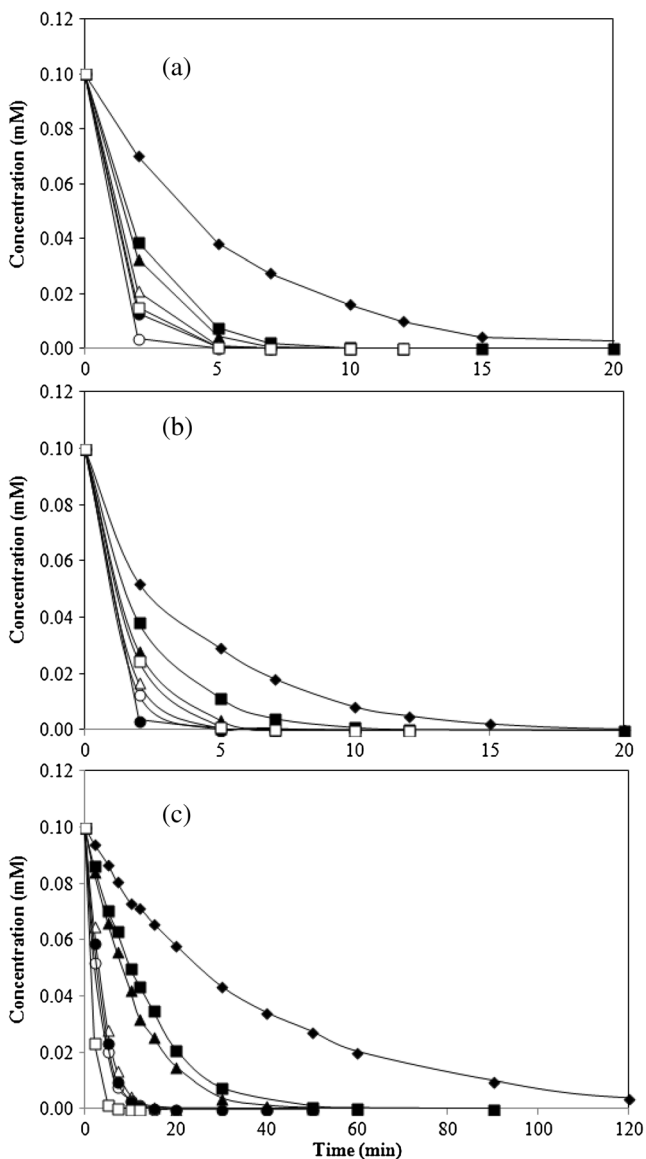
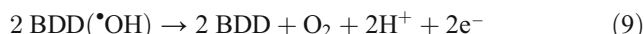


Fig. 1 The effect of the applied current on the oxidative degradation of ICP with time in **a** EF-Pt **b** EF-BDD and **c** AO-BDD systems. *I* (mA): 50 (filled diamonds), 100 (filled squares), 200 (filled triangles), 300 (white triangles), 400 (white circles), 500 (filled circles), 1000 (white squares). [IMC]=0.1 mM, [Na₂SO₄]=50 mM, [Fe²⁺]=0.2 mM, pH=3.0, V=200 mL, O₂ flow rate=1 L min⁻¹

EF-Pt (Fig. 1a) and EF-BDD (Fig. 1b), the time needed for complete disappearance of ICP was short due to higher production of [•]OH with increasing applied current up to 400 and 500 mA, respectively. For example, ICP was completely removed at 50, 20, 12, 10, and 7 mins for 50-, 100-, 200-, 300-, and 400-mA applied currents in EF-Pt cell. Further increase in applied current did not result to high degradation rate for ICP in EF-Pt and EF-BDD cells due to parasitic reactions (5)–(8) consuming [•]OH or BDD([•]OH) (reaction (9)). These reactions involved the destruction of hydroxyl radicals either with H₂O₂, HO₂[•], or Fe²⁺ (reactions (5)–(7)), the dimerization of hydroxyl radical to H₂O₂ (reaction (8)) in

bulk solution, and the oxidation of BDD([•]OH) to O₂ which takes place at the anode according to reaction (9) and H₂ evolution at the cathode (reaction (10)) (Brillas et al. 2009; Panizza and Cerisola 2009; Martínez-Huitle and Brillas 2009; Hammami et al. 2007).



The degradation kinetics of ICP exhibited in Figs. 1a–c showed that the time needed for complete disappearance of ICP at the same applied current was defined as follows for cell configuration employed: EF-Pt < EF-BDD < AO-BDD. For instance, the complete removal of ICP at 100-mA constant current was at 20, 30, and 90 min in EF-Pt, EF-BDD, and AO-BDD cells, respectively. The oxidation efficiency of AO-BDD seems to be lower compared to EF process. This behavior is especially significant at low-applied current, and can be explained by the production of supplementary [•]OH in the bulk solution in the case of EF process (Sirés et al. 2007a, b). The oxidation reaction is limited to the anode surface that constitutes another restriction for AO (Dirany et al. 2010).

Fig. 1 shows that decreasing in ICP concentration by time was exponential in all cases highlighting that the oxidation follows a pseudo-first-order kinetics (Brillas et al. 2009; Dirany et al. 2010; Beltran-Heredia et al. 2001). Indeed, the degradation of ICP by hydroxyl radicals can be described by second-order kinetics:



With [•]OH being a very reactive species and having very short lifetime, the quasi-stationary state hypothesis can be applied to the concentration of [•]OH, therefore, it can be written:

$$-d[\text{ICP}]/dt = k_{\text{abs}(\text{ICP})}[\text{•OH}][\text{ICP}] = k_{\text{app}(\text{ICP})} \times [\text{ICP}] \quad (12)$$

with $k_{\text{app}(\text{ICP})} = k_{\text{abs}(\text{ICP})}[\text{•OH}]$. Then, the integrated form of Eq. (12) can be written as:

$$\ln(C_0/C_t) = k_{\text{app}} \times t \quad (13)$$

The apparent rate constants $k_{\text{app}(\text{ICP})}$ for different current values were determined from slope of the straight lines of the graphs in Fig. 1 according to Eq. (13) and were given in

Table 2. As can be seen in Fig. 1, the decay of ICP with $\cdot\text{OH}$ radicals fits to the pseudo first-order reaction kinetics model. The correlation coefficients obtained from this kinetics model were greater than 0.99 for all current values (Brillas et al. 2009; Panizza and Cerisola 2009) that indicated the oxidation of ICP was diffusion-controlled (Dirany et al. 2010).

When the current increased from 50 to 400 mA in Pt-EF and 50 to 500 mA in EF-BDD cells, apparent rate constants (k_{app}) values increased; however, further increases in current values results in decreases in k_{app} values due to parasitic reactions (5)–(9) discussed above. Another reason might be reduction of H_2O_2 at the cathode by reaction (13) that affected the production rate of $\cdot\text{OH}$ through Fenton reaction (2). Consequently, 400- and 500-mA applied currents can be considered as optimal current values for EF-Pt and EF-BDD cells, respectively.



Note also that k_{app} values in EF-Pt and EF-BDD processes were similar at low current values but they were differed each other upper 300 mA. On the other hand, the rate constants obtained in EF process with both anodes were found to be very high compared to anodic oxidation (AO-BDD) (Table 2).

When the current values increased from 50 to 1,000 mA, k_{app} values increased (Table 2). Whereas optimal current values in EF-Pt and EF-BDD cells are observed at 400 and 500 mA, respectively.

Effect of catalyst concentration

One of the main advantages of the EF system is that the catalyst (Fe^{2+} ions) is continuously regenerated by the reduction of Fe^{3+} formed from Fenton reaction (reaction (2)) at carbon felt cathode according to reaction (4). Thus, the Fe^{2+} ions are continuously present in the solution promoting the formation of $\cdot\text{OH}$ through the Fenton reaction in the bulk solution (Hammami et al. 2007).

Table 2 Apparent rate constant k_{app} (min^{-1}) values as a function of applied current for ICP in EF-Pt, EF-BDD, and AO-BDD cells

Current (mA)	EF-Pt		EF-BDD		AO-BDD	
	k_{app}	R^2	k_{app}	R^2	k_{app}	R^2
50	0.213	0.997	0.262	0.997	0.027	0.999
100	0.557	0.999	0.474	0.996	0.099	0.993
200	0.676	0.997	0.715	0.998	0.118	0.994
300	0.950	0.994	0.971	0.996	0.330	0.992
400	1.451	0.996	1.037	0.995	0.351	0.997
500	1.001	0.997	1.584	0.999	0.377	0.995
1,000	0.961	0.994	0.759	0.993	0.831	0.999

To assess the optimal concentration of catalyst (Fe^{2+}) for efficient degradation, the oxidation of ICP was conducted at different Fe^{2+} concentration. Firstly, degradation procedure was applied to ICP aqueous solutions in which ferrous ion concentration ranged from 0.05 to 1.0 mM in EF-Pt cell. The decay of ICP was followed by HPLC analysis and obtained results were given in Fig. 2. The results showed that the fastest ICP degradation was obtained in 0.2-mM Fe^{2+} . For these different Fe^{2+} concentrations, kinetic analysis following pseudo-first reaction allowed to determine k_{app} values according to Eq. (12) as 0.30, 0.34, 0.55, 0.19, 0.16 min^{-1} , respectively, for the initial Fe^{2+} concentrations (Fig. 3). As can be seen in Fig. 3, the k_{app} value obtained in 0.2-mM Fe^{2+} was higher than the others. Thus, Fe^{2+} concentration of 0.2 mM can be adapted for the oxidation of ICP in EF-Pt and EF-BDD cells. This value is in agreement with several reports of Oturan's group demonstrating that the optimal catalyst concentration for EF process with CF cathode ranged between 0.1–0.2 mM (Brillas et al. 2009; Hammami et al. 2007). These concentrations constitute critical value to avoid parasitic reaction (7) (Brillas et al. 2009).

Determination absolute rate constant for oxidation of ICP

The absolute rate constant of the reaction between ICP and $\cdot\text{OH}$ was evaluated by the method of competition kinetics using the 4-hydroxybenzoic acid (4-HBA) as standard competitor, since its absolute rate constant ($k_{abs(4-HBA)} = 2.19 \times 10^9 \text{ L mol}^{-1} \text{ s}^{-1}$) was well established (Beltran-Heredia et al. 2001). The electro-Fenton treatment of an aqueous solution initially containing ICP and 4-HBA at same concentration of 0.1 mM was carried out at 50 mA using EF-Pt cell. The concentration decay of both compounds was measured by HPLC over a short period at the beginning of the treatment to avoid the interference of formed intermediates.

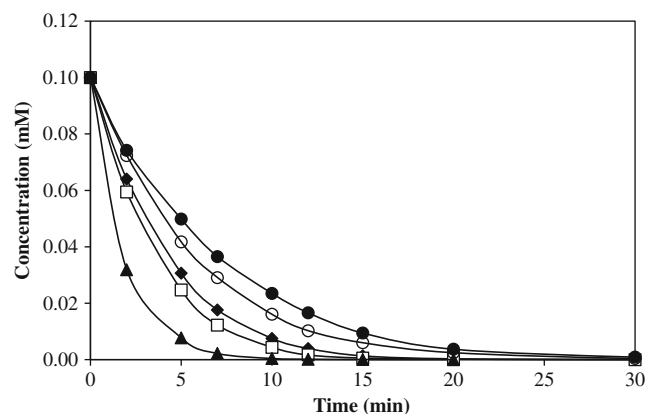


Fig. 2 Effect of Fe^{2+} concentration on the degradation of ICP with time in EF-Pt. [Fe^{2+}] (mM): 0.05 (filled diamonds), 0.1 (white squares), 0.2 (filled triangles), 0.5 (white circles), 1.0 (filled circles) [ICP]=0.1 mM, [Na_2SO_4]=50 mM, pH=3.0, V=200 mL, I=100 mA, O_2 flow rate=1 L min^{-1}

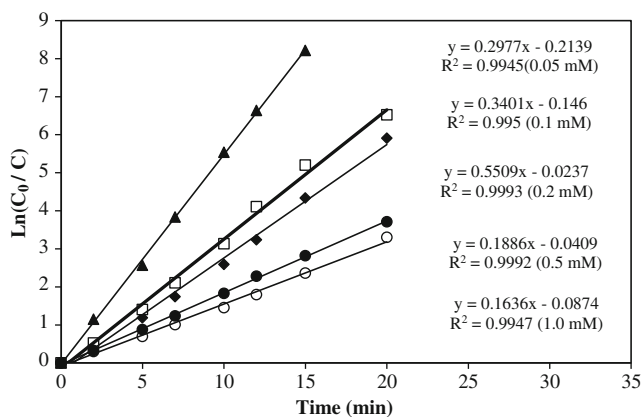


Fig. 3 Determination apparent rate constants (k_{app}) for different catalyst (Fe^{2+}) concentration on the degradation of ICP with time in EF-Pt. [Fe^{2+}] (mM): 0.05 (filled diamonds), 0.1 (white squares), 0.2 (filled triangles), 0.5 (filled circles), 1.0 (white circles) [ICP]=0.1 mM, [Na_2SO_4]=50 mM, pH=3.0, V=200 mL, I=100 mA, O_2 flow rate=1 L min^{-1}

The degradation of ICP and 4-HBA by hydroxyl radicals can be described by second-order kinetics:

$$-d[\text{ICP}]/dt = k_{abs(\text{ICP})}[\cdot\text{OH}][\text{ICP}] = k_{app(\text{ICP})} \times [\text{ICP}] \quad (15)$$

$$-d[4\text{-HBA}]/dt = k_{abs(4\text{-HBA})}[\cdot\text{OH}][4\text{-HBA}] = k_{app(4\text{-HBA})} \times [4\text{-HBA}] \quad (16)$$

The apparent rate constants $k_{app(\text{ICP})}$ and $k_{app(4\text{-HBA})}$ can be determined from the slope of the straight lines obtained from integrated forms of Eqs. (15) and (16), as 0.088 and 0.157 min^{-1} , respectively.

Under these conditions, ICP and 4-HBA compete to react with $\cdot\text{OH}$. Combination of integrated equations from Eqs. (15) and (16) permits to calculate the absolute rate constant for ICP as follows:

$$k_{abs(\text{ICP})} = k_{abs(4\text{-HBA})} \left\{ k_{app(\text{ICP})} / k_{app(4\text{-HBA})} \right\} \quad (17)$$

In this sense, kinetic analysis for the competitive pseudo-first-order reaction of ICP and 4-HBA for EF process was done and the results were given in Fig. 4. The absolute rate constant was then obtained from Eq. (15) and found to be $k_{abs(\text{ICP})} = 1.23 \times 10^9 \text{ L mol}^{-1} \text{ s}^{-1}$.

TOC removal efficiency

To assess the mineralization efficiency of different cell configurations, electrolysis of 0.1-mM ICP aqueous solution at 400 mA was monitored by measuring the total organic carbon (TOC) removal. The treatment was conducted over 8 h and TOC values were analyzed at 2, 4, 6, and 8 h for EF-Pt, EF-BDD, and AO-BDD cells. Comparative TOC removal percentage values for three cell configurations were given in Fig. 5. As can be observed on Fig. 5, the TOC removal was

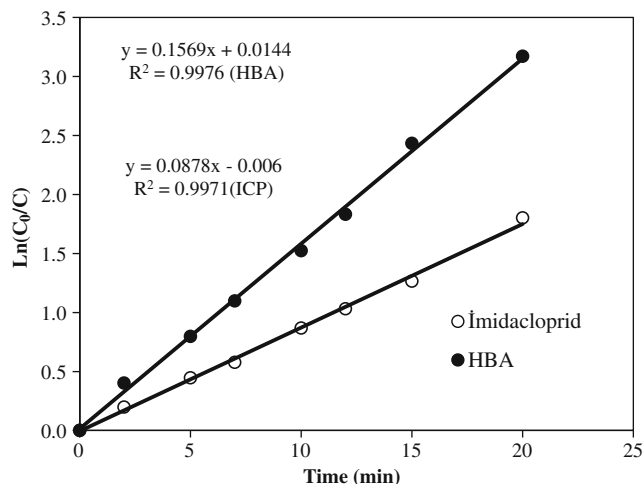


Fig. 4 Kinetic analysis for the determination of absolute rate constant of the reaction between ICP and $\cdot\text{OH}$ in EF-Pt taking 4-HBA as standard competitor. ICP (white circles) and HBA (filled circles), [ICP]=0.1 mM, [4-HBA]=0.1 mM, [Fe^{2+}]=0.2 mM, [Na_2SO_4]=50 mM, pH=3.0, I=50 mA, V=200 mL, O_2 flow rate=1 L min^{-1}

rather high at the end of the first 2 h for both BDD and Pt anode. Overall mineralization of the solution, in terms of TOC removal, was obtained after 2 h of treatment in EF-BDD and AO-BDD cells, while the mineralization degree remained at 71 % in EF-Pt cell. At the end of 8-h treatment, TOC removal efficiency of 0.1-mM ICP solution in EF-Pt, EF-BDD, and AO-BDD was 91, 96, and 93 %, respectively. These results showed that BDD anode was more efficient than Pt anode in EF. The advantage of AO-BDD and EF-BDD over EF-Pt cell can be attributed to the efficient of mineralization of carboxylic acids (Oturán et al. 2011; 2012) by more reactive BDD($\cdot\text{OH}$), since these compounds are resistant to mineralization by homogeneous $\cdot\text{OH}$ in EF-Pt cell (Brillas et al. 2009; Sirés et al. 2007b; Dirany et al. 2010; Oturán et al. 2012).

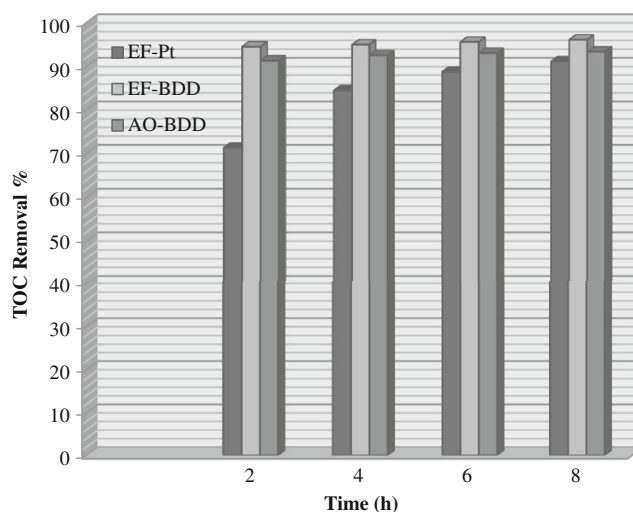


Fig. 5 Comparative TOC removal percentage evolution during the degradation of ICP with time in EF and AO: [ICP]=0.1 mM, [Na_2SO_4]=50 mM, [Fe^{2+}]=0.2 mM, pH=3.0, V=200 mL, I=400 mA, O_2 flow rate=1 L min^{-1}

Several works has been published in literature for the degradation of ICP by using different methods because of the adverse effect of this insecticide on the environment. These methods especially focused on heterogeneous and homogeneous photocatalysis of ICP. The comparison of the present study with those obtained by other AOPs highlight clearly the outstanding removal/mineralization efficiency of EF process with BDD anode (Table 3).

Identification of carboxylic acids

It is well known that the AOPs lead to the formation of new organic products such as aromatic by-products and short-chain carboxylic acids before complete mineralization. These aliphatic (RH) or aromatic (ArH) compounds can be destroyed in their turn by homogenous $\cdot\text{OH}$ (in the bulk solution) (Eq. (18) or (19)):



To identify and quantify the generated short-chain carboxylic acids during electro-Fenton process, 0.1-mM ICP aqueous solution was treated at 400 mA constant current by EF-Pt system and analyzed by ion-exclusion chromatography. The formation of formic, acetic, oxalic, and glyoxylic acids were detected at 16.4, 18.0, 8.3, and 11.3-min retention times, respectively (Fig. 6). As can be seen in Fig. 6, these carboxylic acids were reached to their maximum concentration of 0.31, 0.25, 0.15, and 0.10 mM at 50, 60, 90, and 15 min, respectively, and then their concentrations decreased gradually under action of homogenous $\cdot\text{OH}$ in the bulk solution and completely mineralized after 8 h, except oxalic and glyoxylic acids were remained very low concentration levels even after 8-h treatment.

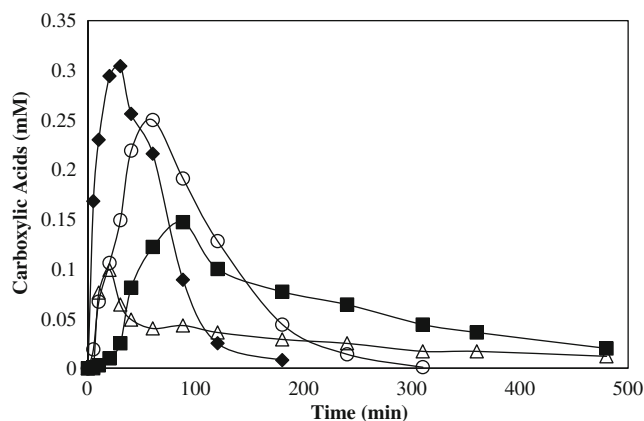


Fig. 6 Evolution of carboxylic acids during the degradation of ICP with time in EF-Pt. Oxalic acid (filled squares), formic acid (filled diamonds), glyoxylic acid (white triangles), acetic acid (white circles), [ICP]=0.1 mM, $[\text{Na}_2\text{SO}_4]=50$ mM, $[\text{Fe}^{2+}]=0.2$ mM, pH=3.0, V=200 mL, I=400 mA, O_2 flow rate=1 L min^{-1}

Identification and evolution of inorganic ions

The evolution of released inorganic ions (Cl^- , NO_3^- , NH_4^+) during EF treatment of 0.1-mM ICP was followed by ionic chromatography analysis. The evolution with time of released inorganic ions during electrolysis by EF-Pt system at 400-mA constant current is shown in Fig. 7. ICP chemical structure includes one Cl and five N atoms, the maximum limits of Cl and N to be released into the solution were 0.1 and 0.5 mM, respectively. Figure 7 shows that the maximum concentration of Cl^- was reached at 30 min. Contrary to Cl^- , the mass balance was not reached for N. The total amount of NO_3^- and NH_4^+ was equal to the 0.35 mM at 8 h. The N mass balance of N has been generally not complete during AOPs (Almeida et al. 2012). The lost of N can be explained by potential formation of gaseous products like N_2 or N_xO_y . Chlorine was easily transformed quantitatively to Cl^- at 120 min and its concentration remained almost constant since, in contrast to BDD anode, Pt anode was not able to oxidize efficiently Cl^- to Cl_2 (Brillas et al. 2009; Dirany et al. 2012).

Table 3 Comparison of the mineralization efficiency between results obtained in this study and those reported already by using other AOPs for the treatment of ICP aqueous solutions

Authors	Degradation method	Processing time (min)	TOC removal (%)	COD removal (%)	DOC removal (%)
Malato and Caceres (2001)	Photo-Fenton	187	90	–	–
Malato and Caceres (2001)	Photocatalysis	421	90	–	–
Moza et al. (1998)	Photolysis	240	90	–	–
Segura et al. (2008)	Photo-Fenton	70	66	80	–
Mahmoodi et al. (2007)	Nano-photocatalysis	240	–	92	–
Philippidis et al. (2009)	Photo-electrocatalysis	1,080	–	–	66
This study	Electro-Fenton	120	94	–	–
This study	Anodic oxidation	120	91	–	–

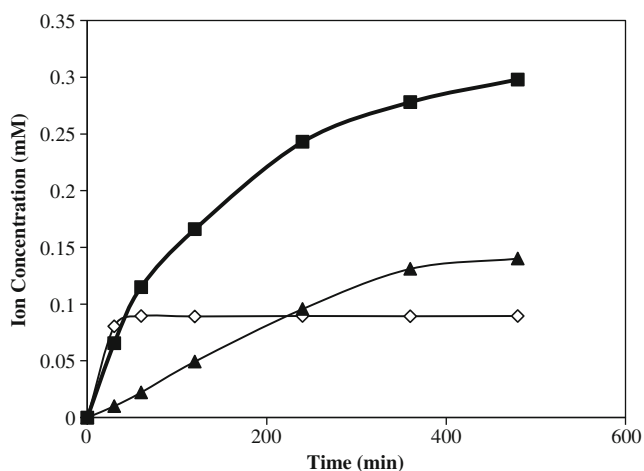


Fig. 7 Evolution of inorganic ions during degradation of ICP with time in EF-Pt. Cl^- (white diamonds), NO_3^- (filled squares), NH_4^+ (filled triangles), $[\text{ICP}]=0.1 \text{ mM}$, $[\text{K}_2\text{SO}_4]=50 \text{ mM}$, $[\text{Fe}^{2+}]=0.2 \text{ mM}$, $\text{pH}=3.0$, $V=200 \text{ mL}$, $I=400 \text{ mA}$, O_2 flow rate= 1 L min^{-1}

Mineralization pathway of ICP during EF treatment

Different oxidation intermediates of ICP were identified during its oxidation in water or organic solvents by photocatalytic degradation, photodegradation, and ozonation was given in literature (Moza et al. 1998; Dell’Arciprete et al. 2009;

Scippers and Schwack 2008; Malato and Caceres 2001; Kitsiou et al. 2009; Bourgin et al. 2011). It is interesting to compare the formed reaction intermediates and degradation mechanisms between the AOPs and EF process. For that, we identified eight aromatic oxidation intermediates formed at different time intervals (5, 7, and 10 min) during the EF treatment of the ICP by LC/ESI-MS/MS and GC/MS analyses. Based on the results obtained, we proposed a plausible degradation/mineralization pathway for ICP by $\cdot\text{OH}$ (Fig. 8). In the initial solution before electrolysis for ICP, M^+ ions were observed together with sodium adducts as $(\text{M} + \text{Na})^+$ at m/z 278 in mass spectra by LC-ESI/MS/MS. The sodium sulfate was added to medium as the electrolyte. The analysis of the samples taken within the first 10 min indicated that $\cdot\text{OH}$ attacks took place in two different regions: (i) $\cdot\text{OH}$ attacks to N- NO_2 position on the imidazolidine group of ICP. The loss of $-\text{NO}_2$ group yields the compounds **I** (2-chloropyridine (2-ethylamino)-N-oxomethaniminium), **II** (1-((6-chloropyridin-3yl) methyl) N-oxoimidazolidine-2-iminium) and **III** (1-((6-chloropyridin-3yl)methyl) 2-(hydroxyimino)-imidazolidine-1-ium). The $-\text{NO}_2$ group oxidized then to NO_3^- ion. Its time-dependent increase was given in Fig. 8. Compound **I** undergoes then ring opening reaction at the level of the imidazoline group. In addition, the oxidation of $\text{C}=\text{N}-\text{NO}_2$ by $\cdot\text{OH}$ leads to the formation

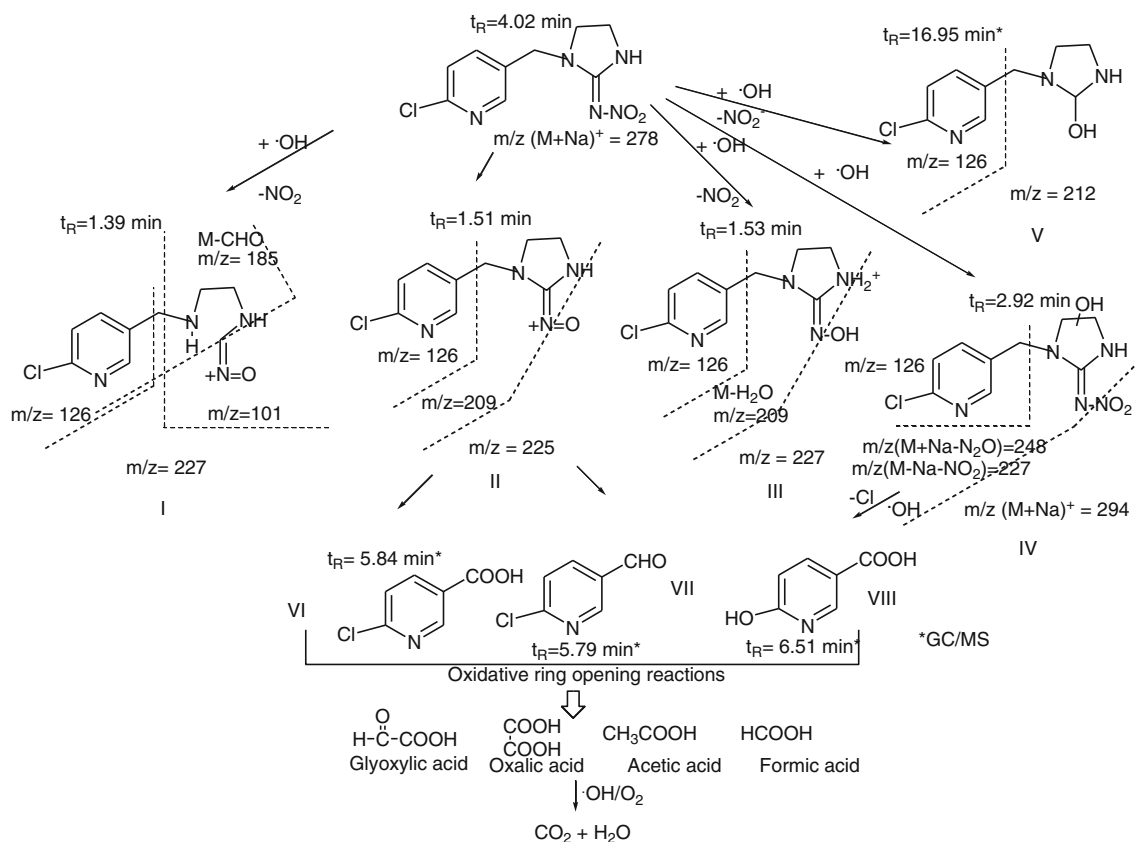


Fig. 8 Proposed mineralization pathway for ICP mineralization by $\cdot\text{OH}$ generated during EF process

of compound **V** (1-((6-chloropyridin-3-yl) methyl) imidazolidine-2-ol) by loss of $-\text{NO}_2^-$ group. (ii) Addition of $\cdot\text{OH}$ on the imidazolidine ring allows formation of compound **IV** (1-((6-chloropyridine-3-yl) methyl-hydroxy)-imidazolidin-2-ylidene nitramide). Further oxidation of compounds **I–V** by $\cdot\text{OH}$ with bond breaking between imidazolidine and 2-chloropyridine group leads to compounds 6-chloronicotinic acid (**VI**), 6-chloronicotinaldehyde (**VII**), and 6-hydroxynicotinic acid (**VIII**) which were detected at m/z 157, 141, and 139 by GC/MS, respectively. The carboxylic acids identified and followed during the treatment were formed by oxidative ring opening reactions of these latter compounds.

Conclusions

The EF and AO processes were applied for the oxidative degradation of ICP by using carbon felt cathode, and Pt and BDD anodes. The results showed that BDD anode was significantly more efficient than Pt anode in EF processes due to the generation of large amount of active BDD($\cdot\text{OH}$) radicals in the case of the former anode. The EF process with BDD anode showed outstanding removal/mineralization efficiency in the treatment of ICP synthetic solutions. The kinetics analysis, based on the concentration decay of ICP, showed that the oxidation of ICP by hydroxyl radical was in good agreement with pseudo-first-order reaction. Using competition kinetics method, the absolute rate constant of reaction between ICP and $\cdot\text{OH}$ was found to be $1.23 \times 10^9 \text{ L mol}^{-1} \text{ s}^{-1}$. This reaction order implies that the oxidation was diffusion-controlled. The optimal catalyst concentration in EF treatment of ICP was found as 0.2 mM. Optimal applied current was evaluated as 400 and 500 mA for Pt-EF and BDD-EF cells configurations. Formic, acetic, oxalic, and glyoxylic acids were identified as end-products before mineralization. The initial chlorine and organic nitrogen present in ICP were also converted to Cl^- and $\text{NO}_3^-/\text{NH}_4^+$ /gaseous product, respectively, during treatment. The degradation products of ICP in EF were analyzed by GC/MS and LC/ESI-MS/MS, and eight main intermediates were determined. Finally, according to identified aromatic and aliphatic intermediates, released inorganic ions, and TOC removal results, a plausible mineralization pathway for ICP by $\cdot\text{OH}/\text{BDD}(\cdot\text{OH})$ was proposed.

References

- Almeida LC, Garcia-Segura S, Arias C, Bocchi N, Brillas E (2012) Electrochemical mineralization of the azo dye acid red 29 (chromotrope 2R) by photoelectron-Fenton process. *Chemosphere* 89:751–758
- Anhalt JC, Moorman TB, Koskinen WC (2007) Biodegradation of imidacloprid by an isolated soil microorganism. *J Environ Sci Heal B* 42:509–514
- Banks KE, Hunter TDH, Wachal DJ (2005) Diazinon in surface waters before and after a federally mandated ban. *Sci Total Environ* 350: 86–93
- Beltran-Heredia J, Torregrosa J, Domínguez JR, Peres JA (2001) Kinetic model for phenolic compound oxidation by Fenton's reagent. *Chemosphere* 45:85–90
- Benitez FJ, Real FJ, Acero JL, Garcia C, Llanos EM (2007) Kinetics of phenylurea herbicides oxidation by Fenton and photo-Fenton processes. *J Chem Technol Biot* 82:65–73
- Bourgin M, Violleau F, Debrauwerd L, Albeta J (2011) Ozonation of imidacloprid in aqueous solutions: reaction monitoring and identification of degradation products. *J Hazard Mater* 190:60–68
- Boye B, Dieng MM, Brillas E (2002) Degradation of herbicide 4-chlorophenoxyacetic acid by advanced electrochemical oxidation methods. *Environ Sci Technol* 36:3030–3035
- Brillas E, Sirés I, Oturan MA (2009) Electro-Fenton process and related electrochemical technologies based on Fenton's reaction chemistry. *Chem Rev* 109:6570–6631
- Cernigoj U, Stangar UL, Trebs P (2007) Degradation of neonicotinoid insecticides by different advanced oxidation processes and studying the effect of ozone on TiO_2 photocatalysis. *Appl Catal B Environ* 75:229–238
- Cox C (2001) Imidacloprid *J Pestic Reforms* 21:15–21
- Daneshvar N, Aber S, Khani A, Khataee AR (2007) Study of imidacloprid removal from aqueous solution by adsorption onto granular activated carbon using an on-line spectrophotometric analysis system. *J Hazard Mater* 144:47–51
- Daneshvar N, Aber S, Vatanpour V, Rasoulifard MH (2008) Electro-Fenton treatment of dye solution containing orange II: influence of operational parameters. *J Electroanal Chem* 615:165–174
- Dell'Arciprete ML, Santos-Juanes L, Sanz AA, Vicente R, Amat AM, Furlong JP, Martire DO, Gonzalez MC (2009) Reactivity of hydroxyl radicals with neonicotinoid insecticides: mechanism and changes in toxicity. *Photochem Photobiol Sci* 8:1016–1023
- Diagne M, Oturan N, Oturan MA (2007) Removal of methyl parathion from water by electrochemically generated Fenton's reagent. *Chemosphere* 66:841–848
- Dirany A, Sirés I, Oturan N, Oturan MA (2010) Electrochemical abatement of the antibiotic sulfamethoxazole from water. *Chemosphere* 81:594–602
- Dirany A, Sirés I, Oturan N, Özcan A, Oturan MA (2012) Electrochemical treatment of sulfachloropyridazine: kinetics, reaction pathways, and toxicity evolution. *Environ Sci Technol* 46: 4074–4082
- EU Directive 2000/60/EC of the Council and the European Parliament of 23 October 2000, OJL 237.
- Endocrine disruptor Screening Program: Tier 1 Screening Order Issuing Announcement. Federal Register Notice, Oct 21, 2009. Vol. 74, No. 202, pp. 54422–54428.
- Flox C, Ammar S, Arias C, Brillas E, Vargas-Zavala AV, Abdelhedi R (2006) Electro-Fenton and photoelectro-Fenton degradation of indigo carmine in acidic aqueous medium. *Appl Catal B Environ* 67:93–104
- Guan H, Chi D, Yu J, Li X (2008) A novel photodegradable insecticide: preparation, characterization and properties evaluation of nano imidacloprid. *Pestic Biochem Phys* 92:83–91
- Hammami S, Oturan N, Bellakhal N, Dachraoui M, Oturan MA (2007) Oxidative degradation of direct orange 61 by electro-Fenton process using a carbon felt electrode: application of the experimental design methodology. *J Electroanal Chem* 610:75–84
- Ishii Y, Kobori I, Araki Y, Kuroguchi S, Iwaya K, Kagabu S (1994) HPLC determination of the new insecticide Imidacloprid (chloronicotiny insecticides), and its behavior in rice and cucumber. *J Agric Food Chem* 42:2917–2921

- Kitsiou V, Filippidis N, Mantzavinos D, Poullos I (2009) Heterogeneous and homogeneous photocatalytic degradation of the insecticide imidacloprid in aqueous solutions. *Appl Catal B Environ* 86:27–35
- Kopling DW, Thurman EM, Goosby DA (1996) Occurrence of selected pesticides and their metabolites in near-surface aquifers of the Midwestern United States. *Environ Sci Technol* 30:335–340
- Mahmoodi NM, Arami M, Limaee NY, Gharanjig K (2007) Photocatalytic degradation of agricultural *N*-heterocyclic organic pollutants using immobilized nanoparticles of titania. *J Hazard Mater* 145:65–71
- Malato S, Caceres DJ (2001) Degradation of imidacloprid in water by photo-Fenton and TiO₂ photocatalysis at a solar pilot plant: a comparative study. *Environ Sci Technol* 35:4359–4366
- Marselli B, Garcia-Gomez J, Michaud PA, Rodrigo MA, Comminellis C (2003) Electrogeneration of hydroxyl radicals on boron-doped diamond electrodes. *J Electrochem Society* 150:79–83
- Martínez-Huitle CA, Brillas E (2009) Decontamination of wastewaters containing synthetic organic dyes by electrochemical methods: a general review. *Appl Catal B Environ* 87:105–145
- Martínez-Huitle CA, Ferro S (2006) Electrochemical oxidation of organic pollutants for the wastewater treatment: direct and indirect processes. *Chem Soc Rev* 35:1324–1340
- Martins AF, da S, Frank C, Wilde ML (2007) Treatment of a trifluraline effluent by means of oxidation-coagulation with Fe(VI) and combined Fenton processes. *Clean-Soil, Air, Water* 35:88–99
- Meyer MT, Thurman EM (1996) Herbicide metabolites in surface water and ground water. *ACS Symposium Series 630*; American Chemical Society, Washington, DC, p 318
- Michaud PA, Panizza M, Ouattara L, Diaco T, Foti G, Comminellis C (2003) Electrochemical oxidation of water on synthetic boron-doped diamond thin film anodes. *J Appl Electrochem* 33:151–154
- Moza PN, Hustert K, Feicht E, Kettrup A (1998) Photolysis of imidacloprid in aqueous solution. *Chemosphere* 36:497–502
- Nidheesh PV, Gandhimathi R (2012) Trends in electro-Fenton process for water and wastewater treatment: an overview. *Desalination* 299:1–15
- Oturan MA (2000) An ecologically effective water treatment technique using electrochemically generated hydroxyl radicals for in situ destruction of organic pollutants: application to herbicide 2,4-D. *J Appl Electrochem* 30:477–482
- Oturan MA, Guivarch E, Oturan N, Sirés I (2008) Oxidation pathways of malachite green by Fe³⁺-catalyzed electro-Fenton process. *Appl Catal B Environ* 82:244–254
- Oturan N, Hamza M, Ammar S, Abdelhdi R, Oturan MA (2011) Oxidation/mineralization of 2-nitrophenol in aqueous medium by electrochemical advanced oxidation processes using Pt/carbon-felt and BDD/carbon-felt cells. *J Electroanal Chem* 661:66–71
- Oturan N, Brillas E, Oturan MA (2012) Unprecedented total mineralization of atrazine and cyanuric acid by anodic oxidation and electro-Fenton with a boron-doped diamond anode. *Environ Chem Lett* 10:165–170
- Ozcan A, Şahin Y, Koparal AS, Oturan MA (2008) Degradation of picloram by the electro-Fenton process. *J Hazard Mater* 153:718–727
- Ozcan A, Şahin Y, Koparal AS, Oturan MA (2009) A comparative study on the efficiency of electro-Fenton process in the removal of prothion from water. *Appl Catal B Environ* 89:620–626
- Pandey G, Dorrian SJ, Russell RJ, Oakeshott JG (2009) Biotransformation of the neonicotinoid insecticides Imidacloprid and thiamethoxam by *Pseudomonas* sp. 1G. *Biochem Biophys Res Comm* 380:710–714
- Panizza M, Cerisola G (2009) Direct and mediated anodic oxidation of organic pollutants. *Chem Rev* 109:6541–6569
- Philippidis N, Sotiropoulos S, Efstathiou A, Poullos I (2009) Photoelectrocatalytic degradation of the insecticide imidacloprid using TiO₂/Ti electrodes. *J Photochem Photobiol A Chem* 204:129–136
- Rouvalis A, Karadima C, Zioris IV, Sakkas VA, Albanis T, Iliopoulou-Georgudaki J (2009) Determination of pesticides and toxic potency of rainwater samples in western Greece. *Ecotox Environ Safe* 72:828–833
- Scippers N, Schwack W (2008) Photochemistry of imidacloprid in model systems. *J Agric Food Chem* 56:8023–8029
- Segura C, Zaror C, Mansilla HD, Mondaca MA (2008) Imidacloprid oxidation by photo-Fenton reaction. *J Hazard Mater* 150:679–686
- Sirés I, Garrido JA, Rodríguez RM, Cabot PL, Centellas F, Arias C, Brillas E (2006) Electrochemical degradation of paracetamol from water by catalytic action of Fe²⁺, Cu²⁺, and UVA light on electrogenerated hydrogen peroxide. *J Electrochem Soc* 153:D1–D9
- Sirés I, Centellas F, Garrido JA, Rodríguez RM, Arias C, Cabot PL, Brillas E (2007a) Mineralization of clofibrac acid by electrochemical advanced oxidation processes using a boron-doped diamond anode and Fe²⁺ and UVA light as catalysts. *Appl Catal B Environ* 72:373–381
- Sirés I, Arias C, Cabot PL, Centellas F, Garrido JA, Rodríguez RM, Brillas E (2007b) Degradation of clofibrac acid in acidic aqueous medium by electro-Fenton and photoelectro-Fenton. *Chemosphere* 66:1660–1669
- Sirés I, Guivarch E, Oturan N, Oturan MA (2008) Efficient removal of triphenylmethane dyes from aqueous medium by in situ electrogenerated Fenton's reagent at carbon-felt cathode. *Chemosphere* 72:592–600
- Suchail S, Guez D, Belzunces LP (2011) Discrepancy between acute and chronic toxicity induced by imidacloprid and its metabolites in *Apis mellifera*. *Environ Toxicol Chem* 20:2482–2486
- Wamhoff H, Schneider V (1999) Photodegradation of imidacloprid. *J Agric Food Chem* 47:1730–1734
- Zahoor M, Mahramanlioglu M (2011) Adsorption of imidacloprid on powdered activated carbon and magnetic activated carbon. *Chem Biochem Eng Quarterly* 25:55–63
- Zapata A, Velegriaki T, Sanchez-Perez JA, Mantzavinos D, Maldonado MI, Malato S (2009) Solar photo-Fenton treatment of pesticides in water: effect of iron concentration on degradation and assessment of ecotoxicity and biodegradability. *Appl Catal B Environ* 88:448–454
- Zapata A, Malato S, Sánchez-Pérez JA, Oller I, Maldonado MI (2010) Scale-up strategy for a combined solar photo-Fenton/biological system for remediation of pesticide-contaminated water. *Catal Today* 151:100–106